

Electronic confinement on stepped Cu(111) surfaces: *Ab initio* studyP. A. Ignatiev,¹ V. S. Stepanyuk,¹ A. L. Klavsyuk,¹ W. Hergert,² and P. Bruno¹¹Max-Planck-Institut für Mikrostrukturphysik, Weinberg 2, D-06120 Halle, Germany²Fachbereich Physik, Martin-Luther-Universität, Halle-Wittenberg, Friedemann-Bach-Platz 6, D-06099 Halle, Germany

(Received 7 November 2006; revised manuscript received 22 February 2007; published 24 April 2007)

The state-of-the-art *ab initio* calculations are performed to study surface states on stepped Cu(111) surfaces with the terrace widths ranging from 12 to 21 Å. In agreement with experiments of Hansmann *et al.* [Phys. Rev. B **67**, 121409(R) (2003)], close to the Fermi energy we reveal electronic states significantly affected by repulsive potential at steps. Our calculations demonstrate that the position of such states is strongly dependent on the terrace width. By using the Kronig-Penney model and *ab initio* results, the strength of potential barriers at step edges is determined. It is shown that the strength of the confining barriers on Cu(111) vicinals can be significantly affected by decoration of step edges with monatomic Fe wires, similar to recent experimental findings of Shiraki *et al.* [Phys. Rev. Lett. **92**, 096102 (2004)]. Spin-dependent scattering of surface electrons at Fe wires is shown to result in the formation of spin-polarized surface states on stepped Cu(111) surfaces. The majority states remain unaffected. A localization of the minority states at Fe wires suppresses the confinement-like features of the local density of states.

DOI: 10.1103/PhysRevB.75.155428

PACS number(s): 73.20.At, 73.21.-b, 71.15.Ap

Vicinal surfaces of noble metals¹ have been the object of intense research for the past decade.²⁻¹⁰ This particular interest is determined by several reasons. On the one hand, vicinal surfaces are very suitable objects for studying low-dimensional nanostructures: they can be used as templates to grow one-dimensional (1D) wires.^{11,12} On the other hand, noble-metal surfaces support Shockley surface states. These electronic states arise in the inverted L gap of a metal band; they are well localized in the direction perpendicular to the surface and exhibit dispersive quasi-two-dimensional (quasi-2D) free-electron-like behavior.¹³ Surface states scatter strongly at point defects, steps, etc., forming standing waves, which can be observed by means of scanning tunneling microscopy (STM) and/or scanning tunneling spectroscopy (STS) and studied using *ab initio* methods.¹⁴⁻¹⁶ Quasi-2D surface states are confined within parallel steps. This was obviously demonstrated by Bürgi *et al.*³ They built a quantum resonator from two perfectly straight and parallel steps on Ag(111) surface, measured the local density of states (LDOS) inside it, and explained their results by a simple Fabry-Pérot-like model. They also demonstrated that the resonator was decoupled from its surrounding through the absorption of surface-state electrons at steps. The coupling of surface-state electrons to the bulk states can be rationalized by the strength of confining potentials at the step edges. In this manner, vicinal surfaces can be treated as an array of confining potentials. Due to the surface-bulk coupling, the strength of confining potentials depends on the exact structure of a vicinal surface. There is no such coupling on the flat (111) substrate, and the coupling is small for vicinal surfaces with a rather large terrace width. In this case, potential barriers are large, all the terraces are decoupled, surface-state electrons are confined to the terraces, and each step can be treated as a quantum well (QW).^{3-6,10} The coupling of surface states with bulk states increases when the terraces get narrower.⁶ This results in the reduction of confining potentials, and surface-state electrons can propagate above the vicinal surface.⁴⁻⁶ On Cu(111) vicinals, the switch from the propagating states to the QW states starts at the terrace width

around 17 Å.⁴⁻⁶ It should be noted that such transition runs continuously. Both of these states have the band bottom shifted toward higher energies. While partially confined propagating states have dispersive bands, QW states exhibit a quantized band structure with a number of distinctively visible energy levels. All these features were observed by means of angle-resolved photoemission spectroscopy (ARPES) and STM and/or STS.^{2,4-6,8,17}

Hansmann *et al.* studied surface states on Cu(111) vicinals in the transition region by means of STS and/or STM.⁸ They performed measurements on surfaces with the terrace width ranging from 16 up to 70 Å. The analysis of their results yields two common features in all measured spectra: the first is surface-state-like onset of the spectra and the second is a broad but very distinct peak. The surface-state-like onset indicates that Cu(111) extended 2D surface states still exist on the considered vicinal surfaces, only partially affected by the finite transparency of the step superlattice. The second feature, i.e., the peak, can originate either from a collective coupling of propagating states to barriers at all the steps or from local confinement of surface electrons to the terraces. The peak should appear at the same energy for all terraces if the overall “superlattice” effect dominates. Experiments, however, revealed a clear dependence of the peak position on the terrace width, even if measurements were performed at adjacent terraces with different widths. This suggests that the peak is formed by states the properties of which are determined by local confinement on a single terrace.

In the presence of adsorbates on stepped surfaces, interesting phenomena can occur. Equidistant steps of vicinal surfaces provide a natural pattern for self-assembling low-dimensional nanostructures. Adsorbates diffusing across terraces of a vicinal surface can be trapped in the potential minimum at the steps, forming structures of 1D nature. In particular, Fe stripes were observed on Cu(111) (Ref. 11); Co wires are reported to grow on Pt(997).¹² Magnetic properties of such low-dimensional nanostructures significantly depend on various conditions and are the focus of research.¹⁸⁻²⁰ On the other hand, such nanostructures may affect a confining

potential at steps of vicinal surface, changing surface states. For instance, CO molecules adsorbed at step edges significantly reduce confining potentials.⁷ Shiraki *et al.* have recently reported on the same effect of Fe adatoms on surface states of Au(111) vicinals.^{9,21} They fabricated Fe nanowires at the steps of the vicinal Au(111) surfaces and examined the surface electronic structure at room temperature by means of ARPES. A set of QW levels typical to strongly confined states was revealed on clean Au(788). This picture remains unaffected until the coverage of evaporated Fe is less than 0.04 monolayer, but then changes dramatically. Instead of the set of QW levels, ARPES measurements demonstrated a peak with a parabolic dispersion. It is suggested that Fe wires attached to the Au steps behave as attractive scatterers, leading to the reduction of the repulsive potential at steps.

Our work is inspired by papers of Hansmann *et al.*⁸ and Shiraki *et al.*⁹ At first, we investigate surface states of clean Cu(111) vicinals by means of the *ab initio* Korringa-Kohn-Rostoker (KKR) Green's function method. Then we proceed to the study of Cu(111) vicinals decorated with Fe wires and demonstrate that localization of the minority surface-state electrons at Fe wires results in the formation of spin-polarized surface states.

The *ab initio* calculations are performed within the framework of the local-density approximation of the density-functional theory (DFT) using the KKR Green's function method.^{22,23} The key point of such an approach is that the solution of the Kohn-Sham equations (and therefore the ground-state density) can be formulated in terms of Green's function.²³ The Green's function of a perturbed system can be found from that of the reference (unperturbed) system by means of the Dyson equation. If there is a translational symmetry in the system, the Dyson equation can be written in the momentum-space representation. Since a surface is treated as a 2D perturbation of the infinite bulk,²⁴ it is possible to calculate spectral density maps (SDM's) as a separate contribution at each point of the Brillouin zone to the entire Green's function.²⁵ The detailed description of the theoretical background of the KKR Green's function method and its applications can be found elsewhere.^{26–28} Herein we briefly list the features of the particular KKR method realization we use. In our calculations, potentials are assumed to be spherically symmetric inside the Wigner-Seitz sphere³⁰ (atomic sphere approximation), but a full charge density is used. Integration over the energy is made in a complex plane, because in this case the Green's function is smooth and it allows to reduce the integrating mesh significantly.³¹ Although DFT does not account for properties of dynamical origin, it is an accurate method to determine static quantities.²⁹ Thermal fluctuation may act to destroy a static magnetic order in the absence of an external field. However, if fluctuations are rather slow, nanowires would behave as magnetic ones for many practical purposes.³² For example, Gambardella *et al.*³³ have demonstrated that Co atomic chains on Pt(111) exhibit ferromagnetic long-range order owing to the presence of anisotropy barriers.

First, we consider surfaces vicinal to Cu(111), namely, Cu(332), Cu(775), Cu(443), Cu(997), and Cu(554). Figure 1(a) depicts the LDOS calculated above the terrace center of the considered surfaces. They can be directly compared with

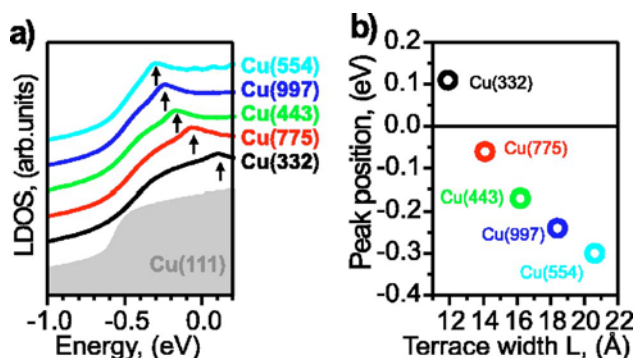


FIG. 1. (Color online) (a) The LDOS calculated at the center of terraces of Cu(332), Cu(775), Cu(443), Cu(997), and Cu(554) stepped surfaces. The LDOS on flat Cu(111) surface is shown as well. Two features of the LDOS on Cu(111) vicinals are visible: the upward shift of surface-state onset and a broad, but evident peak marked with arrows. With the increase of the terrace width, the peak moves to lower energies. The peak position versus terrace width is plotted in (b).

LDOS calculated on flat Cu(111) surface, which is marked in Fig. 1(a) by the shaded area. The LDOS onset corresponds to the surface-state band bottom. A brief analysis of Fig. 1(a) reveals that surface states of Cu(111) vicinal surfaces are shifted toward higher energies in comparison to the flat Cu(111). A similar effect has been observed in the STS experiments of Sánchez *et al.*² and Hansmann *et al.*⁸ The calculated LDOS of vicinal surfaces has another important feature. One can see broad but evident peaks similar to those observed by Hansmann *et al.* In Fig. 1(a), these peaks are marked by arrows. Such a peak is not observed in the LDOS of flat Cu(111) and its position strongly depends on a terrace width. For instance, the peak is unoccupied on Cu(332) ($L = 11.9$ Å), but it shifts under the Fermi level on Cu(775) ($L = 14.1$ Å). The peak position versus the terrace width is plotted in Fig. 1(b). Our results are in good agreement with the STS measurements.⁸ In particular, for Cu(443) and Cu(554), the calculated peak positions are equal respectively -0.17 and -0.3 eV, and corresponding experimental values are approximately -0.15 and -0.25 eV. It is important to note here that STS experiments were performed on a vicinal surface with inequivalent terraces of different widths. The overall superlattice effect is, hence, suppressed and the peak positions are determined by local confinement. As a result, one can observe shifts of the peak position even at adjacent terraces with different widths.⁸ Our *ab initio* results are obtained for the infinite array of the equivalent terraces separated by steps. Such a system actually should be treated as a superlattice, and hence, the contribution to the peak of the overall effect of all the confining potentials is significant. The ratio of contributions to the LDOS peak arising due to local confinement and overall superlattice effect can be rationalized in terms of the strength of confining potential at the step edges. It can be done within the 1D Kronig-Penney model.^{2,34}

The simplest form of the 1D Kronig-Penney (KP) model is derived if we consider the steps as a periodic array of δ -function potentials with the barrier strength U_0a .³⁵ In this

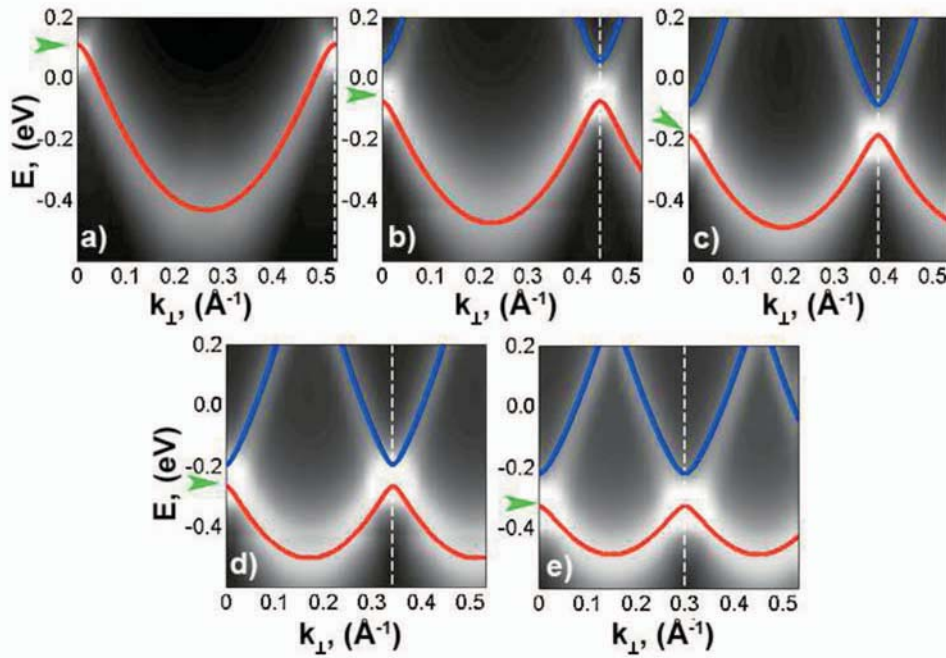


FIG. 2. (Color) Spectral density maps of (a) Cu(332), (b) Cu(775), (c) Cu(443), (d) Cu(997), and (e) Cu(554) surfaces calculated using KKR Green's function method. Bands are back folded exactly at boundaries of superlattice Brillouin zone (reciprocal vectors $k_{\perp} = \pi/L$ are marked with the vertical dashed white lines). The 1D KP model bands are drawn by lines on the top of the spectral density maps: red solid curves correspond to the first band of 1D KP approximation, blue solid curves correspond to the second one. The green arrows correspond to the energies of the LDOS peaks.

case, the dispersion relation for the electrons on vicinal surfaces can be written in terms of energy as

$$E(k_{\perp}) = \hbar^2/(2m^*L^2)[\cos^{-1}(|T|\cos(k_{\perp}L)) - \phi]^2 + E_0, \quad (1)$$

where L is the terrace width, k_{\perp} is the wave-vector component parallel to the surface and perpendicular to the steps, m^* is the effective mass of the surface-state electrons, and E_0 is the bottom of the surface states on the infinite (111) surface. The module of energy-dependent transmission coefficient $|T|$ and phase shift ϕ can be obtained using the potential barrier strength U_0a as $|T|^2 = 1/[1 + (q_0/q)^2]$ and $\phi = -\tan^{-1}(q_0/q)$, where $q = \sqrt{(2m^*/\hbar^2)(E - E_0)}$ and $q_0 = (m^*/\hbar^2)U_0a$. The described model has only one adjustable parameter, which is the potential barrier strength U_0a . It can be expressed using Eq. (1) through the shift of the surface-state band bottom.

To obtain surface-state band bottoms, we plot SDM's calculated at the center of all the considered terraces. They are shown in Figs. 2(a)–2(e). The boundaries of the superlattice Brillouin zone (reciprocal vectors $k_{\perp} = \pi/L$) are marked in Figs. 2(a)–2(e) with vertical dashed white lines. The bands are back folded exactly at these positions. Since the KKR Green's function method does not operate with wave functions and the bands cannot be obtained explicitly, the surface-state band bottom should be extracted from the SDM's by the fitting procedure. This procedure is based on the fact that SDM reaches its local maximum at the band. At first, for a set of a fixed k_{\perp} , we determine such local maxima of the SDM. Because we use rather dense energy mesh, such energies can be found accurately enough by means of parabolic interpolation of SDM data in the vicinity of its maximum value. Then we fit the obtained band by a polynomial function of k_{\perp} and extract the band bottom energy as the minimum value of the polynomial. The resulting error is estimated to be within several meV. It should be emphasized that this simple procedure can be successfully applied for the

interpolation of the band alone, but can yield wrong results in the case of a complicated band structure.

The KP bands constructed according to the dispersion relation (1) are visualized in Figs. 2(a)–2(e) upon the corresponding SDM's. The first KP bands fit the *ab initio* SDM's surprisingly good, but it is evident that the 1D KP model gives increased gaps at $k_{\perp} = n\pi/L$ for all examined surfaces. It can be explained by neglecting in this model the coupling between surface and bulk states which takes place at the step edges. Energies of the LDOS peaks are marked in Figs. 2(a)–2(e) with green arrows. It is clear that the LDOS peaks are determined by areas of increased spectral density (bright white spots) situated at the gap edges of the 1D KP model. Such behavior of LDOS for 1D KP model was predicted by Davis *et al.*³⁴ The potential barrier strength U_0a calculated from Eq. (1) is plotted in Fig. 3 as a function of the terrace width with solid circles. The values determined by Sánchez *et al.*² and Hansmann *et al.*⁸ are also shown in Fig. 3. In agreement with available experimental data, the barrier strengths are around 1 eV Å and display a growth for smaller terrace widths.⁶ One can see that the barrier strength exhibits the minimum approximately at the terrace width equal to 18 Å. The increase of the barrier strength at large value of the terrace width assumes that surface states get more confined to the terrace, and therefore, it can be treated as the evidence of the transition in the character of the states.

Let us now turn to the results on decorated Cu(111) vicinals. We performed calculations for Cu(332), Cu(775), Cu(443), Cu(997), and Cu(554) surfaces decorated with monatomic Fe wires. The total LDOS calculated at the center of terraces are shown in Fig. 4(a). The peaks marked in Fig. 4(a) by arrows are blurred but still visible and there is a downward shift of the LDOS onset. To get a deeper insight into the effect of Fe wires on surface-state electrons, we investigate the minority and majority LDOS. As an example, the minority and majority LDOS calculated at the center of

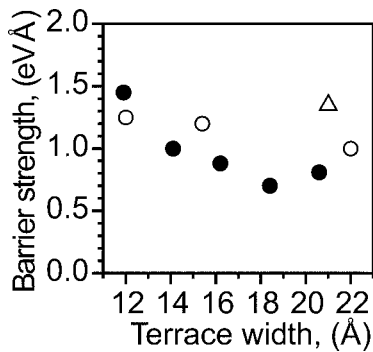


FIG. 3. Dependence of the step barrier strength U_0a on the terrace width. The calculated values are drawn with solid circles. The open circles and the triangle correspond to the values calculated by Sánchez *et al.* (Ref. 2) and by Hansmann *et al.* (Ref. 8). This dependence is in qualitative agreement with available experimental data (Ref. 6). The minimum at 18 Å can be explained by the increased role of local confinement for larger terrace widths, and therefore can be treated as the evidence of the transition in the character of the surface states (Refs. 4–6).

Cu(443) surface terrace are shown in Fig. 4(b). They can be compared with a LDOS of the clean Cu(443) surface, which is marked in Fig. 4(b) by the shaded area. It is evident that the surface states on decorated Cu(111) vicinals become spin polarized. The majority LDOS coincides with the LDOS of the clean Cu(443) almost one to one, but the minority LDOS is different: there is a blurred minimum, but the majority states peak at -0.3 eV and a new broad peak appears at -0.6 eV. As follows from Fig. 5(a), the density of the minority surface states at -0.6 eV is a maximum near the Fe wires and decreases at the center of the terrace. The LDOS calculated at the step of Cu(554) surface (1), at the center of Cu(554) terrace (2), at the step edge (3), and at the Fe wire (Fe) are plotted in Fig. 5(b). The peak at Fe wires is deter-

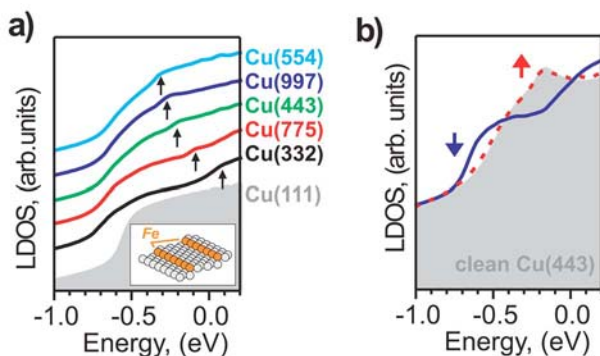


FIG. 4. (Color online) (a) The total LDOS calculated at the center of terraces of Cu(332), Cu(775), Cu(443), Cu(997), and Cu(554) stepped surfaces decorated with monatomic Fe wires. The LDOS on flat Cu(111) surface is drawn with the shaded area. The peak features marked with arrows are less pronounced on clean vicinal surfaces. (b) The spin-polarized LDOS calculated at the center of the terrace of the decorated Cu(443) surface. The majority LDOS (dashed curve) remains unaffected in comparison to the LDOS on clean Cu(443) terrace. The minority LDOS (solid curve) exhibits a broad peak at -0.6 eV.

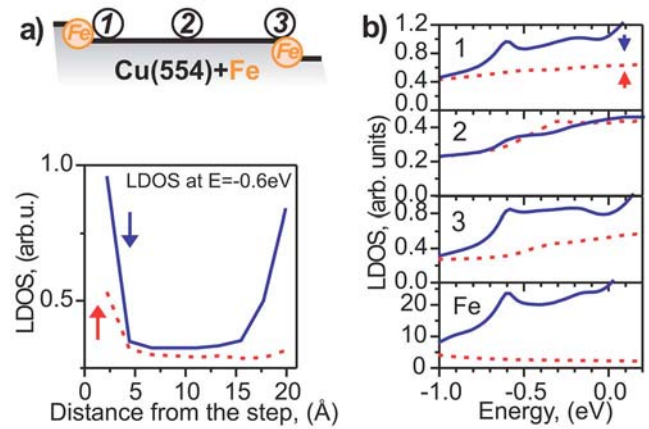


FIG. 5. (Color online) (a) Spatial changes of the minority (solid curve) and majority (dashed curve) LDOS at the peak energy ($E=-0.6$ eV) along the terrace of Cu(554) surface with Fe wires. (b) The spin-polarized LDOS calculated near the step (1), at the center of the terrace (2), at the step edge (3), and at Fe wires (Fe). The minority peak at -0.6 eV is most pronounced in the vicinity of Fe wires and gets blurred at the center of the terrace. The peak at Fe wires is determined by d states and is not affected by the terrace width.

mined by d states and is not affected by the terrace width. Such a picture suggests the localization of the minority surface-state electrons at the Fe wires. On the other hand, Gauyacq *et al.*³⁶ have shown that localized states splitting off the surface-state band bottom should appear whenever the surface-state continuum is perturbed by an attractive potential, so one can expect that the majority states should also be localized as was demonstrated for adatoms on the flat Cu(111) surface.^{37–39} But there is no clear evidence of localization of the majority electrons in Fig. 4(b). To explain this discrepancy, we should stress that Fe wires can significantly modify the overlap between bulk and surface states. Exchange splitting of Fe electronic states may result in a spin-dependent surface-bulk overlap and, hence, in different minority and majority surface electronic states. To confirm this idea, we studied the majority and minority SDM's calculated at the center of the terrace. In both cases, we revealed the 1D KP-like band structure: the majority SDM is the same as the SDM of the corresponding clean vicinal surface; but the band bottom of the minority surface states is situated at -0.6 eV, lower than that on the flat Cu(111). The Fe wire-induced downward shift of the minority surface-state band bottom cannot be adequately treated within the 1D KP model (1). Finally, the localization of the minority states at Fe wires results in depopulation of states with the half wavelength close to terrace width, localized at the center of the terrace. Because these states are situated exactly at the gap edges, a minimum in the minority LDOS appears at the energy of the peak (see Fig. 4).

In conclusion, by means of *ab initio* calculations we have studied clean and decorated Cu(111) vicinals. In agreement with previous experimental works,^{2,4–6,8,17} electronic states significantly affected by repulsive potential at steps have been found close to the Fermi energy. Our calculations have

demonstrated that the position of such states is strongly dependent on the terrace width. The strength of the potential barrier at the step edges has been found to be in good agreement with experimentally determined values.^{2,6,8} It has been shown that decoration of the steps with monatomic Fe rows can significantly affect surface states on vicinal surfaces. Surface states become spin polarized due to spin-dependent

scattering of surface-state and bulk electrons at Fe wires: the majority surface states remain unaffected; the minority states get localized at Fe wires. Such localization suppresses the confinementlike features of LDOS.

This work was supported by Deutsche Forschungsgemeinschaft (DFG SPP 1165).

-
- ¹M. A. Van Hove and G. A. Samoraj, *Surf. Sci.* **92**, 489 (1980).
²O. Sánchez, J. M. García, P. Segovia, J. Alvarez, A. L. Vázquez de Parga, J. E. Ortega, M. Prietsch, and R. Miranda, *Phys. Rev. B* **52**, 7894 (1995).
³L. Bürgi, O. Jeandupeux, A. Hirstein, H. Brune, and K. Kern, *Phys. Rev. Lett.* **81**, 5370 (1998).
⁴J. E. Ortega, S. Speller, A. R. Bachmann, A. Mascaraque, E. G. Michel, A. Närmann, A. Mugarza, A. Rubio, and F. J. Himpsel, *Phys. Rev. Lett.* **84**, 6110 (2000).
⁵F. Baumberger, M. Hengsberger, M. Muntwiler, M. Shi, J. Krem-pasky, L. Patthey, J. Osterwalder, and T. Greber, *Phys. Rev. Lett.* **92**, 196805 (2004).
⁶J. E. Ortega, M. Ruiz-Osés, J. Córdón, A. Mugarza, J. Kuntze, and F. Schiller, *New J. Phys.* **7**, 101 (2005).
⁷F. Baumberger, T. Greber, B. Delley, and J. Osterwalder, *Phys. Rev. Lett.* **88**, 237601 (2002).
⁸M. Hansmann, J. I. Pascual, G. Ceballos, H.-P. Rust, and K. Horn, *Phys. Rev. B* **67**, 121409(R) (2003).
⁹Susumu Shiraki, Hideki Fujisawa, Masashi Nantoh, and Maki Kawai, *Phys. Rev. Lett.* **92**, 096102 (2004).
¹⁰A. Mugarza, J. E. Ortega, F. J. Himpsel, and F. J. García de Abajo, *Phys. Rev. B* **67**, 081404(R) (2003).
¹¹J. Shen, R. Skomski, M. Klaua, H. Jenniches, S. S. Manoharan, and J. Kirschner, *Phys. Rev. B* **56**, 2340 (1997).
¹²P. Gambardella, M. Blanc, L. Bürgi, K. Kuhnke, and K. Kern, *Surf. Sci.* **449**, 93 (2000).
¹³N. Memmel, *Surf. Sci. Rep.* **32**, 91 (1998).
¹⁴V. S. Stepanyuk, L. Niebergall, R. C. Longo, W. Hergert, and P. Bruno, *Phys. Rev. B* **70**, 075414 (2004).
¹⁵V. S. Stepanyuk, L. Niebergall, W. Hergert, and P. Bruno, *Phys. Rev. Lett.* **94**, 187201 (2005).
¹⁶L. Niebergall, V. S. Stepanyuk, J. Berakdar, and P. Bruno, *Phys. Rev. Lett.* **96**, 127204 (2006).
¹⁷F. Baumberger, T. Greber, and J. Osterwalder, *Phys. Rev. B* **64**, 195411 (2001).
¹⁸P. Gambardella, A. Dallmeyer, K. Maiti, M. C. Malagoli, S. Rusponi, P. Ohresser, W. Eberhardt, C. Carbone, and K. Kern, *Phys. Rev. Lett.* **93**, 077203 (2004).
¹⁹J. Dorantes-Davila and G. M. Pastor, *Phys. Rev. Lett.* **81**, 208 (1998).
²⁰J. Dorantes-Davila and G. M. Pastor, *Phys. Rev. B* **72**, 085427 (2005).
²¹S. Shiraki, H. Fujisawa, M. Nantoh, and M. Kawai, *J. Phys. Soc. Jpn.* **74**, 2033 (2005).
²²K. Wildberger, V. S. Stepanyuk, P. Lang, R. Zeller, and P. H. Dederichs, *Phys. Rev. Lett.* **75**, 509 (1995).
²³R. Zeller, P. H. Dederichs, B. Ujfalussy, L. Szunyogh, and P. Weinberger, *Phys. Rev. B* **52**, 8807 (1995).
²⁴K. Wildberger, R. Zeller, and P. H. Dederichs, *Phys. Rev. B* **55**, 10074 (1997).
²⁵N. Papanikolaou, B. Nonas, S. Heinze, R. Zeller, and P. H. Dederichs, *Phys. Rev. B* **62**, 11118 (2000).
²⁶P. Weinberger, *Electron Scattering Theory for Ordered and Disordered Matter* (Oxford University Press, Oxford, 1990).
²⁷J. Zabloudil, R. Hammerling, L. Szunyogh, and P. Weinberger, *Electron Scattering in Solid Matter*, Springer Series in Solid-State Sciences Vol. 147 (Springer, New York, 2005).
²⁸V. Bellini, N. Papanikolaou, R. Zeller, and P. H. Dederichs, *Phys. Rev. B* **64**, 094403 (2001).
²⁹O. Újsághy, J. Kroha, L. Szunyogh, and A. Zawadowski, *Phys. Rev. Lett.* **85**, 2557 (2000).
³⁰S. H. Vosko, L. Wilk, and N. Nusair, *Can. J. Phys.* **58**, 1200 (1980).
³¹K. Wildberger, P. Lang, R. Zeller, and P. H. Dederichs, *Phys. Rev. B* **52**, 11502 (1995).
³²A. Delin, E. Tosatti, and R. Weht, *Phys. Rev. Lett.* **92**, 057201 (2004).
³³P. Gambardella, A. Dallmeyer, K. Maiti, M. C. Malagoli, W. Eberhardt, K. Kern, and C. Carbone, *Nature (London)* **416**, 301 (2002).
³⁴L. C. Davis, M. P. Everson, R. C. Jaklevic, and W. Shen, *Phys. Rev. B* **43**, 3821 (1991).
³⁵R. E. Borland, *Proc. Phys. Soc. London* **77**, 705 (1961).
³⁶J. P. Gauyacq, A. G. Borisov, and A. K. Kazansky, *Appl. Phys. A: Mater. Sci. Process.* **78**, 141 (2004).
³⁷L. Limot, E. Pehlke, J. Kröger, and R. Berndt, *Phys. Rev. Lett.* **94**, 036805 (2005).
³⁸V. S. Stepanyuk, A. N. Klavsyuk, L. Niebergall, and P. Bruno, *Phys. Rev. B* **72**, 153407 (2005).
³⁹B. Lazarovits, L. Szunyogh, and P. Weinberger, *Phys. Rev. B* **73**, 045430 (2006).